Thermal conductivity of MgB_2 in the superconducting state

M. Putti,* V. Braccini, E. Galleani d'Agliano, F. Napoli, I. Pallecchi, and A. S. Siri
INFM-LAMIA/CNR, Dipartimento di Fisica, Via Dodecaneso 33, 16146 Genova, Italy

P. Manfrinetti and A. Palenzona
INFM, Dipartimento di Chimica e Chimica Industriale, Via Dodecaneso 31, 16146 Genova, Italy
(Received 8 October 2002; published 25 February 2003)

We present thermal conductivity measurements on very pure and dense bulk samples, as indicated by residual resistivity values as low as 0.5 $\mu\Omega$ cm and thermal conductivity values higher than 200 W/mK. In the normal state we found that the Wiedemann-Franz law, in its generalized form, works well suggesting that phonons do not contribute to the heat transport. The thermal conductivity in the superconducting state has been analyzed by using a two-gap model. Thanks to the large gap anisotropy we were able to evaluate quantitatively intraband scattering relaxation times of π and σ bands, which depend on the disorder in different way; namely, as the disorder increases, it reduces more effectively the relaxation times of π than that of σ bands, as suggested by a recent calculation [Mazin *et al.*, Phys. Rev. Lett. **89**, 107002 (2002)].

DOI: 10.1103/PhysRevB.67.064505 PACS number(s): 74.25.Fy, 74.70.Ad, 72.15.Eb

I. INTRODUCTION

Since the discovery of MgB_2,[2] experimental findings established a phonon mediated *s*-wave superconductivity. Despite its standard origin, superconductivity in MgB_2 showed several unusual properties that can be ascribed to the presence of two gaps with different amplitudes emphasized by tunneling and specific heat measurements. Theoretical studies[3–5] pointed out that the peculiar electronic structure is the origin of this behavior being the larger gap, Δ_σ, associated with σ bands and the smaller one, Δ_π, associated with π bands. The two-gap model offers a simple explanation of several anomalies in the superconducting state.[6–8] The π and σ bands have different dimensionality, π bands being nearly isotropic, and σ bands two-dimensional, which determines the anisotropy of physical properties. Multiband effects due to the different parity of σ and π bands were predicted in the normal state, too,[1] and, recently, have found confirmation in transport measurements.[9] Since interband impurity scattering turns out to be negligible, different bands behave as separate conduction channels in parallel and either σ or π channel prevails, depending on the disorder degree, being the clean (dirty) samples dominated by π (σ) conduction.

In this paper we present thermal conductivity measurements on bulk samples and we perform a quantitative analysis in the superconducting state to investigate the role of σ and π bands depending on the sample purity.

Thermal conductivity κ in the superconducting state among the other transport properties gives information on quasi-particle (QP) excitations and their dynamics with the advantage of probing only the QP response, since the superfluid does not carry heat. On the other hand, a major complication in the analysis of the thermal conductivity is often a substantial phonon contribution to the heat current. Consequently, the interpretation of experimental data can be ambiguous.

From a basic point of view, QP condensation below T_c causes a decrease of the electron contribution to the thermal conductivity, κ_{el}, and an increase of the phonon contribution, κ_{ph}; thus κ below T_c can show a shoulder or a peak depending on whether the heat current is dominated by electrons or phonons, and a more complex behavior is exhibited when both contributions are important.

From the beginning the thermal conductivity of MgB_2 showed the unexpected feature of not exhibiting any signature of the superconducting transition.[10–13] This "anomaly" was initially ascribed to a perfect compensation of κ_{el} and κ_{ph} (Ref. 11) or to the presence of large thermal resistance at the grain boundaries.[12] As a matter of fact, the discovery that MgB_2 presents two gaps, one of which Δ_π is so small that QP condensation becomes exponential only below a reduced temperature of the order of $t=T/T_c\sim 0.2$, opened new perspectives in the interpretation of thermal conductivity data. Hence, the two gap model successfully used to fit specific heat data[6] can also be applied to the thermal conductivity to estimate the fraction of energy carried by the two bands, providing a useful means to investigate multiband effects.

II. EXPERIMENTAL DETAILS

Dense (up to 2.4 g/cm^3, 90% of the theoretical density), clean and hard cylinder shaped samples have been prepared by a single step method[14] similar to the one reported in Refs. 15 and 16. Amorphous or crystalline B and Mg, put in Ta crucibles welded under argon and closed in quartz tubes under vacuum, were heated up to 950 °C. An x-ray spectrum of a sample prepared by crystalline *B* is shown in Fig. 1. All the peaks associated with the MgB_2 phase are present, no extra peaks due to the presence of free Mg, MgO, are detected. In the inset, SEM (scanning electron microscopy) image of the same sample is shown. The image shows a network of well connected grains ($2-4$ μm large).

Two specimens were prepared for physical measurements: one from crystalline boron (-325 mesh, Alfa Aesar) (MGB-1S), one by using enriched crystalline ^{11}B (-325 mesh, Eagle Picher) (MGB11-1S). The samples were cut in the shape of parallelepiped bar ($1\times 2-3\times 12$ mm^3).

The thermal conductivity was measured using a steady

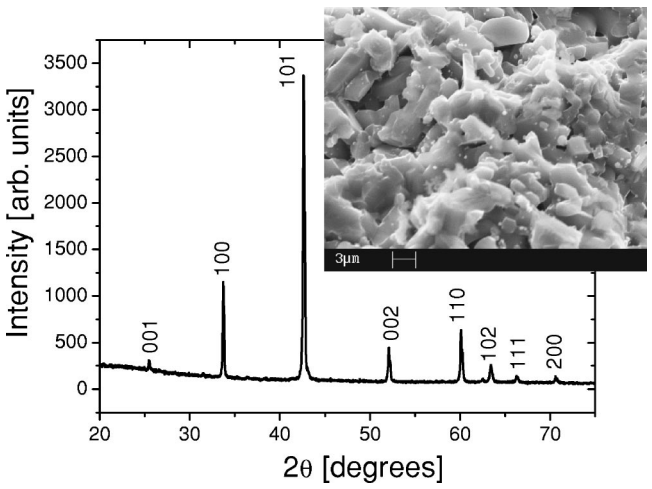

FIG. 1. X-ray pattern diffraction of an enriched ^{11}B bulk sample. The inset shows a SEM image of the same sample. The length scale of the picture is indicated in the bottom.

state flux method with a heat flux sinusoidally modulated at low frequency ($\nu = 0.003 - 0.01$ Hz). Under these conditions the thermal conductivity is extracted as $\kappa = J(\nu)/\nabla T(\nu)$, where $J(\nu)$ is the heat flow provided at the frequency ν and $\nabla T(\nu)$ is the temperature gradient oscillating at the frequency ν. A small resistive heater (1×1 mm^2) is glued by GE varnish on the top end of the bar, being the bottom of the bar thermally connected with the sample holder. In such way a longitudinal heat flow is assured. The gradient applied to the sample was varied from 0.1 to 0.3 K/cm. Seebeck effect was measured simultaneously with the thermal conductivity providing a precise determination of the critical temperature.

III. RESULTS AND DISCUSSIONS

Resistivity measurements of the samples from 30 to 300 K are shown in Fig. 2.

In Table I we report T_c^{onset}, the amplitude of the transition ΔT_c, $\rho(40\text{ K})$ and the residual resistivity ratio defined as RRR $= \rho(300\text{ K})/\rho(40\text{ K})$ for the two samples. The excellent quality of the samples is proved by the high T_c values

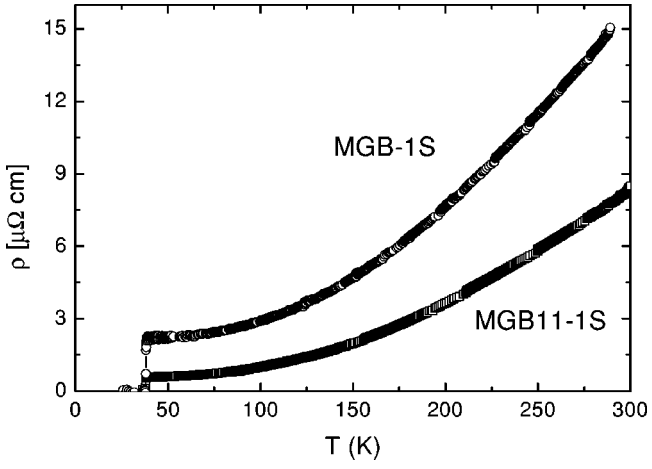

FIG. 2. Resistivity measurements from 40 to 300 K.

TABLE I. Critical temperature T_c^{onset}, amplitude of the transition ΔT_c, $\rho(40\text{ K})$ and residual resistivity ratio defined as RRR $= \rho(300\text{ K})/\rho(40\text{ K})$.

Sample	T_c^{onset} K	ΔT_c K	$\rho(40\text{ K})\,\mu\Omega$ cm	RRR
MGB11-1S	38.7	0.2	0.58	15.3
MGB-1S	38.9	0.3	2.1	7.1

(38.7, 38.9 K), the small ΔT_c values (0.2, 0.3 K), the low values of $\rho(40\text{ K})$ (0.6, 2.1 $\mu\Omega$ cm), and the large values of RRR (15, 7). Between the two samples the enriched ^{11}B (MGB11-1S) has the lower resistivity values which can mainly be ascribed to the very good quality of the Eagle-Picher enriched ^{11}B.[16]

Thermal conductivity measurements of the two samples from 4 to 250 K are shown in Fig. 3. The outstanding quality and high density of the samples is evident from thermal transport properties as well. Indeed, these samples have more than one order of magnitude higher thermal conductivities than sintered samples.[10–12] In particular MGB11-1S exhibits a thermal conductivity as large as 215 W/mK at 65 K, which is nearly two times higher than those of a single crystal,[13] proving the excellent purity and density of this sample.

The thermal conductivity of MGB11-1S increases monotonically in the superconducting state, a change of slope is observable at about 8 K, while no signature of the superconducting transition is present; the normal state curve exhibits a pronounced maximum at about 70 K. Similar behavior is presented by MGB-1S even if only data above 10 K are available.

The normal state behavior of both samples is typical of a good metal in which the electron contribution to heat transport prevails. In order to estimate the relative weight of κ_{el} and κ_{ph} we can consider the effective Lorenz number defined as $\mathcal{L}_{eff} = \kappa\rho/T$. This quantity is assumed equal to $\mathcal{L}_0 = 2.45 \times 10^{-8}$ WΩ K^{-2} by the Wiedemann-Franz law (WFL); in good metals $\mathcal{L}_{eff}$ is equal to $\mathcal{L}_0$ at low temperature where the

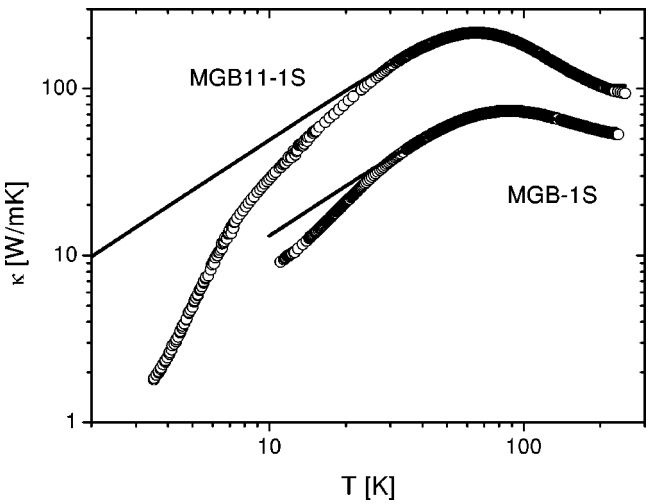

FIG. 3. Thermal conductivity measurements of the samples from 10 to 250 K: the best fitting curves obtained with the parameter values listed in Table II are reported as continuous lines.

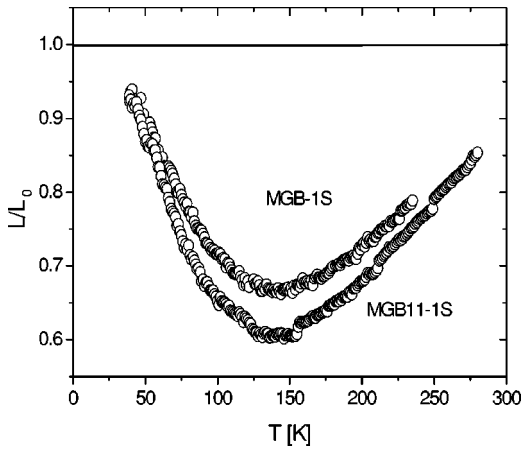

FIG. 4. The effective Lorenz number $\mathcal{L}_{\rm eff}/\leqslant=\kappa\rho/(T\mathcal{L}_0)$ from 40 to 250 K.

electron impurity scattering prevails, then it decreases showing a minimum at about one-tenth the Debye temperature Θ_D, deeper and deeper with increasing sample purity;[17] in dilute alloys where $\kappa_{\rm ph}$ is not at all negligible $\mathcal{L}_{\rm eff}$ becomes larger than $\mathcal{L}_0$ and the ratio $\mathcal{L}_{\rm eff}/\mathcal{L}_0\simeq(1+\kappa_{\rm ph}/\kappa_{\rm el})$ gives information on the relative weight of $\kappa_{\rm el}$ and $\kappa_{\rm ph}$.[18] In Fig. 4 we plot $\mathcal{L}_{\rm eff}/\mathcal{L}_0$ for the two samples from 40 to 250 K. The curves exhibit the typical behavior of good metals with slightly different levels of purity: at low temperatures the curves approach $\mathcal{L}_0$ from below; they show a minimum at around 130 K$\sim 0.1\Theta_D$ (considering that in MgB_2 $\Theta_D \sim 1000$ K—Refs. 19 and 20), which is more pronounced for MGB11-1S; finally, the curves increase toward $\mathcal{L}_0$. Thus, we can conclude that in the normal state the WFL substantially works and $\kappa_{\rm ph}$ can be neglected. Similar results were obtained also in sintered sample with low thermal conductivity,[9] while different conclusions have been drawn on a single crystal,[13] where a violation of the WFL was claimed. Actually, in a small sample with not well defined geometrical shape as a single crystal the geometrical factor which relates conductivity to conductance can be different in thermal and electrical measurement, giving an incorrect evaluation of the Lorenz number. In large bar cut specimens the geometrical factors can be estimated with better precision and more reliable verification of the WFL can be made.

In the superconducting state, since $\kappa_{\rm ph}$ decreases as $(T/\Theta_D)^3$, we can assume that the thermal conductivity is dominated by electrons as well. In the superconducting state, due to QP condensation which decreases $\kappa_{\rm el}$ and enhances $\kappa_{\rm ph}$, their relative weight can change. However, in MgB_2, there is much evidence of the anomalous presence of π-band QP over a wide temperature range below T_c.[6,13] Hence, we assume that lattice vibrations give negligible contribution to the thermal transport in the temperature region of our interest and in the following we analyze the thermal conductivity data in term of the electron contribution only.

The electron thermal conductivity in the superconducting state $\kappa_{\rm el}^S$ can be written as

$$\kappa_{\rm el}^S(T)=\kappa_{\rm el}^n(T)g(t,\alpha), \tag{1}$$

where $\kappa_{\rm el}^n(T)$ is the electron thermal conductivity in the normal state and $g(t,\alpha)$, for a given reduced gap, $\alpha=\Delta(0)/k_BT_c$, and reduced temperature, $t=T/T_c$, takes into account the QP condensation. The function $g(t,\alpha)$ was calculated in the framework of the BCS theory for dominant scattering of the electrons with the impurities,[21] or with the phonons[21,22] reproducing very well thermal conductivity in the low temperature superconductors. To analyze experimental data using Eq. (1) two main problems have to be solved. First, Eq. (1) has to be generalized to multiband conduction; second, $\kappa_{\rm el}^n(T)$ has to be estimated. We start from the latter issue.

At low temperature, if the scattering with impurities dominates, one can write:

$$\mathcal{W}_{\rm el}\simeq\mathcal{W}_{\rm el}^{\rm im}+\mathcal{W}_{\rm el}^{\rm ph}, \tag{2}$$

where the thermal resistance $\mathcal{W}_{\rm el}=1/\kappa_{\rm el}$ is the sum of the thermal resistivity for scattering with impurities, $\mathcal{W}_{\rm el}^{\rm im}$, and for scattering with phonons, $\mathcal{W}_{\rm el}^{\rm ph}$; i.e., one can assume approximate validity of Matthiessen's rule. The first term in Eq. (2) is given by

$$\mathcal{W}_{\rm el}^{\rm im}=\frac{\rho_0}{T\mathcal{L}_0} \tag{3}$$

with $\rho_0^{-1}=\rho_{0,\pi}^{-1}+\rho_{0,\sigma}^{-1}$ being the two-band residual resistivity given by the parallel of residual resistivity of π band, $\rho_{0,\pi}$, and σ band, $\rho_{0,\sigma}$. The second term, following Ref. 17, is given in a single-band case by

$$\mathcal{W}_{\rm el}^{\rm ph}=A\left(\frac{\Theta_D}{T}\right)^2\frac{\rho_{\rm ph}(T)}{T\mathcal{L}_0}, \tag{4}$$

where

$$\rho_{\rm ph}(T)=B\left(\frac{T}{\Theta_D}\right)^5\int_0^{\Theta_D/T}{\rm d}x\,\frac{x^5}{(e^x-1)(1-e^{-x})}.$$

A and B are constants and in our case one should replace their product $A\cdot B$ with an appropriate average over the two bands which we call C. So we write:

$$\mathcal{W}_{\rm el}^{\rm ph}=C\left(\frac{\Theta_D}{T}\right)^3\frac{1}{T\mathcal{L}_0}\int_0^{\Theta_D/T}{\rm d}x\,\frac{x^5}{(e^x-1)(1-e^{-x})}$$

Despite its simplicity, this model describes very well the normal state thermal conductivity of samples with very different degrees of disorder, with reasonable parameter values;[9] it contains the right features, vanishing to zero at low temperature linearly with T and requiring only three free parameters (ρ_0, Θ_D, and C) whose reliability can be checked by resistivity . The best fitting procedure is performed from 40 to 200 K and the curves obtained with the parameter values listed in Table II are reported in Fig. 3 as continuous lines.

The theoretical curves fit the experimental data in the normal state in excellent way, while just below T_c, they lay above the data, decreasing linearly with temperature, where the experimental data start to decrease with larger slopes, due

TABLE II. Values of the parameters Θ_D, ρ_0, and C obtained from the normal state thermal conductivity best fit and α_π, α_σ, and x obtained by fitting Eq. (5) with the superconducting state thermal conductivity.

Sample	Θ_D, K	$\rho 0$ ($\mu\Omega$ cm)	C ($\mu\Omega$ cm K-2)	α_π	α_σ	x
MGB11-1S	1190	0.50	12	0.57	2.17	0.85
MGB-1S	1130	1.9	18	0.60	1.90	0.75

to the QP condensation. In Table II we can see that the Θ_D and C values, which determine the intrinsic term, are nearly the same for both the samples, while the ρ_0 values change by a factor 4, as consequence of the different purity of the two samples; moreover we can see that the ρ_0 values are slightly lower than $\rho(40\ \mathrm{K})$ reported in Table I. Anyway, ρ_0, Θ_D, and C values are in fair agreement with those obtained by fitting resistivity measurements.[9]

Now we address the problem of generalizing Eq. (1) in the case of multiband conduction. Following the approach used for the specific heat,[6] we can write:

$$\frac{\kappa_{\mathrm{el}}^s(T)}{\kappa_{\mathrm{el}}^n(T)} = x g(t,\alpha_\pi) + (1-x) g(t,\alpha_\sigma), \tag{5}$$

where $\alpha_\pi = \Delta_\pi(0)/k_B T_c$ and $\alpha_\sigma = \Delta_\sigma(0)/k_B T_c$; the relative weights x and $(1-x)$ that in Ref. 6 are related to the energy which condenses in each band, in our case rather represent the average energy fractions carried by the π and σ bands respectively; our samples being poly-crystalline, the relative weights take into account the mobility of the carriers in each band averaged in the three directions.

Denoting with $\kappa_\pi^n(T) = x\kappa_{\mathrm{el}}^n(T)$ and $\kappa_\sigma^n(T) = (1-x)\kappa_{\mathrm{el}}^n(T)$ the π and σ bands thermal conductivity in the normal state, Eq. (5) states that the π and σ bands conduction occurs in parallel, as suggested by Ref. 1.

Once a suitable g function is considered Eq. (5) allows to fit the thermal conductivity data in the superconducting state with x, α_π, and α_σ as free parameters. To describe σ and π QP we choose the g function for electron-impurity scattering[21] in agreement with the fact that, below 40 K, $\kappa_{\mathrm{el}}^n(T)$ is dominated by the scattering with impurities. In Fig. 5 we show κ/T in the superconducting state for the two samples. The continuous line represents $\kappa_{\mathrm{el}}^n(T)/T$, the dashed line represents $\kappa_{\mathrm{el}}^s(T)/T$ given by Eq. (5). The parameters obtained with the best fit procedure are summarized also in Table II. We can see that the two-gap model provides an excellent agreement with the experimental data. We find $\alpha_\pi = 0.57$ (or 0.6) and $\alpha_\sigma = 2.17$ (or 1.9) for MGB11-1S (or MGB-1S); these values, which correspond to $\Delta_\pi(0) = 1.9$ (or 2.0) meV and $\Delta_\sigma(0) = 7.2$ (or 6.3) meV, are in agreement with those found by specific heat data $\alpha_\pi \sim 0.6 - 0.65$ and $\alpha_\sigma \sim 1.9 - 2.2$. For the x parameter we find 0.85 and 0.75 for MGB11-1S and MGB-1S, respectively. From the specific heat analysis it comes out that the energy fraction which condenses in each band is roughly the same; thus our results imply that carriers in π bands are more mobile than in σ bands. Our result is in apparent contradiction with that of Ref. 13 which concluded that the mobilities in the π and σ bands are almost equal. Nevertheless, Ref. 13 discussed the conduction within the boron planes, whereas we measure the conduction averaged over all directions; the latter is clearly lower for σ bands because of their two-dimensional nature.

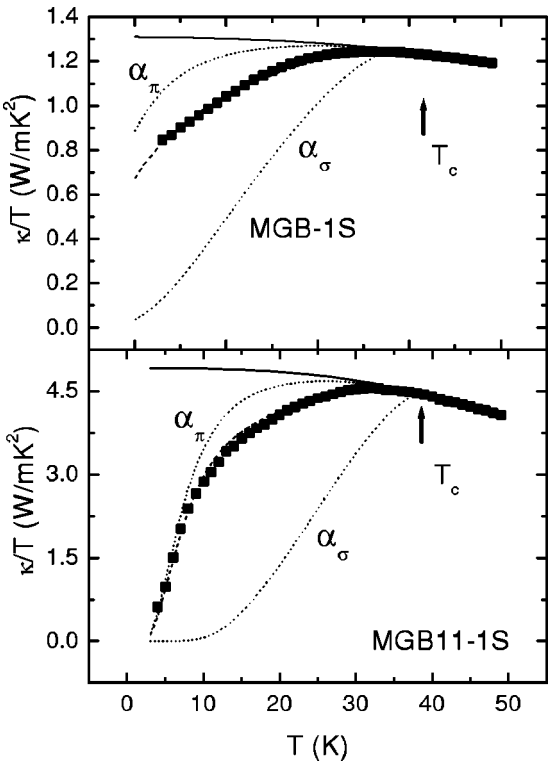

FIG. 5. κ/T in the superconducting state. The continuous line represents the calculated κ_{el}^n/T; the dashed line represents κ_{el}^s/T given by Eq. (5) with the parameter values summarized in Table II; the dotted lines represent κ_{el}^s/T given by Eq. (1) (single-band model) with $\alpha = \alpha_\pi$ and $\alpha = \alpha_\sigma$ given in Table II.

The lacking signature of superconducting transition in thermal conductivity, naturally follows from the two-gap model; in fact, we find that the main contribution to heat transport comes from carriers in π bands whose strong condensation starts for $\alpha_\pi/t \gg 1$ which means $t < 0.2$. In MGB11-1S data a change of slope occurs at about 8 K which in this framework represents the π QP condensation; in fact in Fig. 5 we can see that below 10 K the σ band contribution to $\kappa_{\mathrm{el}}^s(T)/T$ is negligible, and the only π band contribution fits the experimental curve; from 10 K to 40 K also the σ-band contribution is necessary to fit the data.

The right weight of π and σ contributions to transport can be calculated for both samples by $\kappa_\pi^n(T) = x\kappa_{\mathrm{el}}^n(T)$ and $\kappa_\sigma^n(T) = (1-x)\kappa_{\mathrm{el}}^n(T)$ once the reliability of the x and $\kappa_{\mathrm{el}}^n(T)$ evaluation has been verified. We point out that in the fit procedure, slightly varying the gap values, the quality of the fit does not change very much, while the x parameter for both the samples is very well defined. On the other hand, below T_c, $\kappa_{\mathrm{el}}^n(T) = T\mathcal{L}_0/\rho_0$ and therefore it only depends on the residual resistivity ρ_0 which can be experimentally estimated. So we can write:

TABLE III. The intraband scattering time with impurities for π and σ bands, $\tau_\pi^{\rm im}$, $\tau_\sigma^{\rm im}$ and the residual mean free paths $\lambda_{\pi,\sigma} = \tau_{\pi,\sigma}^{\rm im} v_{{\rm F}\pi,\sigma}$ ($v_{{\rm F}\pi} = 5.6\times10^5$ m/s, $v_{{\rm F}\sigma} = 3.2\times10^5$ m/s are the averaged Fermi velocities for π and σ bands—Ref. 7).

Sample	$\tau_\pi^{\rm im}$ (s)	$\tau_\sigma^{\rm im}$ (s)	λ_π (m)	λ_σ (m)
MGB11-1S	2.2×10^{-13}	1.3×10^{-13}	1.2×10^{-7}	4.1×10^{-8}
MGB-1S	0.5×10^{-13}	0.6×10^{-13}	2.9×10^{-8}	1.8×10^{-8}

$$\kappa_\pi^n(T) = \frac{T\mathcal{L}_0}{\rho_{0,\pi}} = x\frac{T\mathcal{L}_0}{\rho_0} = T\mathcal{L}_0\varepsilon_0\omega_\pi^2\tau_\pi^{\rm im}, \tag{6a}$$

$$\kappa_\sigma^n(T) = \frac{T\mathcal{L}_0}{\rho_{0,\sigma}} = (1-x)\frac{T\mathcal{L}_0}{\rho_0} = T\mathcal{L}_0\varepsilon_0\omega_\sigma^2\tau_\sigma^{\rm im}, \tag{6b}$$

where ε_0 is the dielectric constant, $\omega_{\pi,\sigma}$ are the plasma frequencies, and $\tau_{\pi,\sigma}^{\rm im}$ are the intraband scattering relaxation times with impurities for π and σ bands.

Our fits state that carriers in π bands mainly contribute to carry heat. Indeed, the plasma frequency is larger for π than for σ bands[7] and this is enhanced in polycrystalline samples by averaging in the three directions. On the other hand, the scattering relaxation times change from sample to sample. Introducing in Eq. (6) the values of x and ρ_0 listed in Table II, and setting $\omega_\pi = 6.226$ eV and $\omega_\sigma = 3.403$ eV (Ref. 7) we obtain the scattering relaxation times for the two samples summarized in Table III. In particular we find, for the sample MGB11-1S $\tau_\pi^{\rm im} = 2.2\times10^{-13}$ s, $\tau_\sigma^{\rm im} = 1.3\times10^{-13}$ s and the residual mean free paths $\lambda_{\pi,\sigma} = \tau_{\pi,\sigma}^{\rm im} v_{{\rm F}\pi,\sigma}$, where $v_{{\rm F}\pi,\sigma}$ are the averaged Fermi velocities for π and σ bands ($v_{{\rm F}\pi} = 5.6\times10^5$ m/s, $v_{{\rm F}\sigma} = 3.2\times10^5$ m/s[7]), come out $\lambda_\pi = 1.2\times10^{-7}$ m and $\lambda_\sigma = 4.1\times10^{-8}$ m. These values are very large, exceeding the lattice constants by more than two orders of magnitude, indicating the excellent purity of this sample. For MGB-1S the relaxation rates are reduced, but the residual mean free paths are still large ($\lambda_\pi = 2.9\times10^{-8}$m and $\lambda_\sigma = 1.8\times10^{-8}$ m).

Let us now look at the relaxation times in more details. In MGB11-1S $\tau_\pi^{\rm im} > \tau_\sigma^{\rm im}$, while in MGB-1S both the relaxation times are lower and $\tau_\pi^{\rm im} < \tau_\sigma^{\rm im}$. Practically, as the disorder increases, it reduces more effectively $\tau_\pi^{\rm im}$ than $\tau_\sigma^{\rm im}$. Actually, it is not easy to say which kind of disorder is present in MGB-1S, itself being a quite pure sample. But typical defects in MgB_2 are vacancies or substitutions in the Mg site, which form more easily than in the B site. In these cases the relaxation rate for intraband impurity scattering is larger in π than in σ bands ($\tau_\pi^{\rm im} < \tau_\sigma^{\rm im}$).[1] This prediction, which was well verified for large amount of defects,[9] is here confirmed also going from very pure to rather pure samples.

This result can open new perspectives in thermal transport properties. In fact, as the disorder increases, we expect that the transport of σ bands prevails, and in superconducting state, the rapid QP condensation due to the large gap related to σ bands can become evident. Thus, in disordered samples, we expect that the thermal conductivity would diminish in absolute values, but it should show a wide shoulder below T_c. This fact, if true, is quite unusual, in fact the disorder generally smoothens, rather than enhancing features.

As a matter of fact, looking at the thermal conductivity data in literature, polycrystalline sintered samples do not show more evident shoulder than clean samples. We think that polycrystalline samples, that surely are more disordered than single crystals or bulk samples, present resistive grain boundaries, which contribute to the thermal resistance masking the intrinsic behavior of superconducting grains.[12] To emphasize the transport of carriers in σ bands by the progressive inhibition of transport in π bands, it is necessary to gradually introduce defects in pure samples. This can be done by suitable chemical substitution with the advantage of introducing a controlled amount of defects in a chosen site. Up to now, substituted samples have been obtained by sintering powders previously synthesized from the pure elements and such samples are not suitable for transport measurements. A second way is to introduce disorder by irradiation, but in this case the problem is to obtain a uniform defect distribution.

In conclusion, the role of disorder in MgB_2, which multiband effects make so peculiar, has been studied in pure samples by thermal transport measurements. We analyzed in detail the thermal conductivity in the superconducting state, and thanks to the large gap anisotropy we were able to evaluate quantitatively the intraband scattering relaxation times of π and σ bands.

ACKNOWLEDGMENT

This work work is partially supported by the Istituto Nazionale per la Fisica della Materia through the PRA UMBRA.

*Electronic mail address: putti@fisica.unige.it

[1] I. I. Mazin, O. K. Andersen, O. Jepsen, O. Dolgov, J. Kortus, A. A. Golubov, A. B. Kuz'menko, and D. van der Mare, Phys. Rev. Lett. **89**, 107002 (2002).

[2] J. Nagamatsu, N. Nakagawa, T. Muranaka, Y. Zenitani, and J. Akimitzu, Nature (London) **410**, 63 (2001).

[3] A. Y. Liu, I. I. Mazin, and J. Kortus, Phys. Rev. Lett. **87**, 087005 (2001).

[4] H. J. Choi, D. Roundy, H. Sun, M. L. Cohen, and S. G. Louie, Nature (London) **418**, 758 (2002).

[5] H. J. Choi, D. Roundy, H. Sun, M. L. Cohen, and S. G. Louie, Phys. Rev. B **66**, 020513 (2002).

[6] F. Bouquet, Y. Wang, R. A. Fisher, D. G. Hinks, J. D. Jorgensen, A. Junod, and N. E. Phillips, Europhys. Lett. **56**, 856 (2001).

[7] A. Brinkman, A. A. Golubov, H. Rogalla, O. V. Dolgov, J. Kortua, Y. Kong, O. Jepsen, and O. K. Andersen, Phys. Rev. B **65**, 180517 (2002).

[8] A. A. Golubov, A. Brinkman, O. V. Dolgov, J. Kortua, and O. Jepsen, Phys. Rev. B **66**, 054524 (2002).

[9] M. Putti, V. Braccini, E. Galleani d'Agliano, F. Napoli, I. Pallecchi, A. S. Siri, P. Manfrinetti, and A. Palenzona, in Proceedings of BOROMAG, Genoa, 17-19 June 2002, Supercond. Sci. Technol. **16**, 188 (2003).

[10] T. Muranaka, J. Akimitsu, and M. Sera, Phys. Rev. B **64**, 020505 (2001).
[11] E. Bauer, C. Paul, S. Berger, S. Majumdar, H. Michor, M. Giovannini, A. Saccone, and A. Bianconi, J. Phys.: Condens. Matter **13**, L487 (2001).
[12] M. Putti, E. Galleani d'Agliano, D. Marrè, F. Napoli, M. Tassisto, P. Manfrinetti, and A. Palenzona, in *Studies of High temperature Supeconductors*, edited by A. V. Narlikar (Nova Science, New York, 2002), Vol. 38, p. 303.
[13] A. V. Sologubenko, J. Jun, S. M. Kazakov, J. Karpinski, and H. Ott, Phys. Rev. B **66**, 014504 (2002).
[14] A. Palenzona, P. Manfrinetti, and V. Braccini, Tech. Rep., Istituto Nazionale Fisica della Materia (2001), patent, No. TO2001A001098.
[15] D. K. Finnemore, J. E. Ostenson, S. L. Bud'ko, G. Lapertot, and P. C. Canfield, Phys. Rev. Lett. **86**, 2420 (2001).
[16] R. A. Ribeiro, S. L. Bud'ko, C. Petrovic, and P. C. Canfield, cond-mat/0204510.
[17] R. Berman, *Thermal Conduction in Solids* (Clarendon, Oxford, 1976).
[18] M. Putti, in *Studies of High Temperature Superconductors*, edited by A. Narlikar (Nova Science, New York, 2001), Vol. 35, p. 281.
[19] C. Walti, E. Felder, C. Degen, G. Wigger, R. Monnier, B. Delley, and H. R. Ott, Phys. Rev. B **64**, 172515 (2001).
[20] F. Bouquet, R. A. Fisher, N. E. Phillips, D. G. Hinks, and J. D. Jorgensen, Phys. Rev. Lett. **87**, 047001 (2001).
[21] J. Bardeen, G. Rickayzen, and L. Tewordt, Phys. Rev. **113**, 982 (1959).
[22] B. T. Geilikman, M. I. Dushenat, and V. R. Chechetkin, Sov. Phys. JETP **46**, 1213 (1977).